

Inter-Annual Variation and Its Large-Scale Circulation Drivers of October-December Rainfall Onset Date in Tanzania

Juma Saidi Mdelele¹, Guirong Tan²

¹Tanzania Meteorological Authority (TMA), Dar es Salaam, Tanzania

²Nanjing University of Science, Information and Technology (NUIST), Nanjing, China

Email: mdelele@gmail.com

How to cite this paper: Mdelele, J.S. and Tan, G.R. (2025) Inter-Annual Variation and Its Large-Scale Circulation Drivers of October-December Rainfall Onset Date in Tanzania. *Atmospheric and Climate Sciences*, 15, 533-548.

<https://doi.org/10.4236/acs.2025.153027>

Received: March 31, 2025

Accepted: May 20, 2025

Published: May 23, 2025

Copyright © 2025 by author(s) and Scientific Research Publishing Inc.
This work is licensed under the Creative Commons Attribution International License (CC BY 4.0).

<http://creativecommons.org/licenses/by/4.0/>



Open Access

Abstract

This study investigates the inter-annual variation of the October-December (OND) rainfall onset date in Tanzania, including spatial-temporal patterns, atmospheric anomalies, and climatic drivers such as the Indian Ocean Dipole (IOD) and El Niño-Southern Oscillation (ENSO), utilizing daily rainfall data, reanalysis datasets, and climate indices (1993-2023). The onset dates were determined using a threshold-based method, while spatial and temporal variability was analyzed through Empirical Orthogonal Function analysis. Results show that: i) the onset dates were determined using a threshold-based method, while spatial and temporal variability was analyzed through Empirical Orthogonal Function analysis. In Tanzania, there is a unimodal rainfall regime, such as the Southern, Southern Coast, and Southwestern Highlands, rainfall onset typically occurs later, around November or December. ii) Anomalous easterly upper-level winds with convergence and westerly lower-level winds with divergence at low-level, suppress moisture transport with descending over the region will delay rainfall onset during late Onset date (LOD) years. In contrast, the opposite situation will be during Early Onset Date (EOD) years. iii) Both ENSO and IOD have close relationship with the rainfall onset day in Tanzania. Warm SSTA in eastern-central Pacific and western Indian Ocean during El Niño years/positive IOD years, can induce LOD associated circulation patterns and then delay rainfall onset day over most part of the region, especially over east part of the region. However, the warm SSTA in western Pacific to eastern Indian Ocean during La Niña/negative IOD years will induce EOD-like circulation patterns, which will make rainfall onset earlier over most part of the country and the Indian Ocean plays more critical role on the rainfall onset day in Tanzania.

Keywords

Rainfall Onset Day, Indian Ocean Dipole, El Niño/La Niña, Tanzania, Climate Variability

1. Introduction

Climate change has significantly altered global precipitation patterns, affecting rainfall onset, intensity, and duration [1]. Recent studies have documented increased global surface temperatures, with warming over land exceeding that over the oceans [2] [3]. This warming has intensified extreme weather events, including shifts in rainfall onset dates and more frequent droughts and floods [4] [5]. In Africa, climate variability is particularly critical due to the continent's reliance on rain-fed agriculture [6]. Tanzania, a country highly dependent on rain-fed agriculture, faces severe consequences from these climatic shifts. Rainfall pattern disruptions, particularly in the October-December (OND) season, have led to recurrent droughts and floods, significantly affecting agricultural productivity and economic stability [7] [8].

Previous studies have explored climate variability in East Africa (EA), focusing on seasonal rainfall fluctuations and extreme weather events [9] [10]. In particular, studies have highlighted significant shifts in the seasonal timing and intensity of the OND rainfall, revealing a trend toward increased variability. Research by [11] and [12] has shown that the onset and cessation of the OND rainfall season in East Africa, including Tanzania, have become increasingly unpredictable over recent decades. These shifts are linked to large-scale climate drivers such as the ENSO and the IOD. Specifically, ENSO-related sea surface temperature anomalies have been found to affect the timing and intensity of the OND rains, with El Niño events typically leading to early rainfall onset and La Niña events contributing to delays [11]. The IOD also plays a crucial role in modulating rainfall variability in East Africa, with a positive IOD generally leading to above-average rainfall and a negative IOD associated with dry conditions [13] [14].

Further studies, such as those by [15], have documented an increase in the frequency and intensity of extreme weather events in East Africa, including both prolonged dry spells and intense rainfall events during the OND season. These changes have contributed to an increase in rainfall variability, disrupting the regularity and predictability of the rainy season. Additionally, research by [16] suggests that these changes in rainfall patterns are being driven by shifting atmospheric circulation patterns. As a result, the increased variability in rainfall onset, intensity, and duration poses significant challenges for agricultural planning and food security in Tanzania, as farmers increasingly struggle to predict the optimal planting and harvesting windows. These studies underscore the need for more detailed analysis of OND rainfall onset variability and its underlying atmospheric drivers to better inform adaptation strategies in the face of climate change.

However, research on the inter-annual variation of the OND rainfall onset date in Tanzania remains limited. The OND rainfall season plays a vital role in agriculture, with delayed onset date or early cessation impacting crop yields and food security. Despite existing literature linking OND rainfall variability to climatic drivers such as ENSO and IOD [13] [17] [18], their specific influence on onset date variability over Tanzania remains inadequately quantified. Furthermore, the socio-economic consequences of delayed or early OND rainfall onset are under-explored, especially concerning smallholder farmers who rely on precise timing for planting decisions [19]. Given the increasing unpredictability of rainfall patterns due to climate change, improving onset date forecasts could enhance agricultural resilience and disaster preparedness.

This study aims to analyze the inter-annual variability of the onset date during the OND rainfall season in Tanzania, focusing on temporal and spatial variations, circulation anomalies, and key forcing factors. The specific research questions guiding this study include: How does the onset date vary spatially and temporally during the study period (1993-2023)? What are the main forcing factors and circulation anomalies influencing the occurrence of LOD and EOD during the OND rainfall season? How do forcing factors influence the occurrence of LOD or EOD in Tanzania?

This study could benefit policymakers, meteorologists, and agricultural stakeholders by supporting early warning systems and adaptive farming strategies.

2. Materials and Methods

2.1. Study area

The study focuses on the United Republic of Tanzania (URT), situated in East Africa between latitudes 1°S-12°S and longitudes 30°E-40°E as shown in **Figure 1**. Tanzania consists of both the mainland and islands (Zanzibar and Pemba), covering a total area of approximately 945,087 km². According to [20], the country experiences a bimodal rainfall pattern in the northern and eastern regions, with short rains (Vuli) from October to December (OND) and long rains (Masika) from March to May (MAM). The western, southern, and central regions exhibit a unimodal rainfall pattern from October to April or May [21].

2.2. Data

2.2.1. Daily Precipitation Data

Daily precipitation data were obtained from the Climate Hazards Group InfraRed Precipitation with Stations (CHIRPS) dataset, which provides satellite-blended rainfall estimates at a spatial resolution of 0.05° × 0.05° [22]. The dataset spans from January 1, 1993, to December 31, 2023, covering 30 regions in Tanzania. CHIRPS data were accessed from the International Research Institute for Climate and Society (IRI) repository

[<http://iridl.ldeo.columbia.edu/SOURCES/UCSB/CHIRPS/v2p0/daily-improved/global/0p05/prcp/datafiles.html>] and have been validated for East Af-

rica, showing a strong correlation ($r = 0.73$) with gauge-based observations data [23].

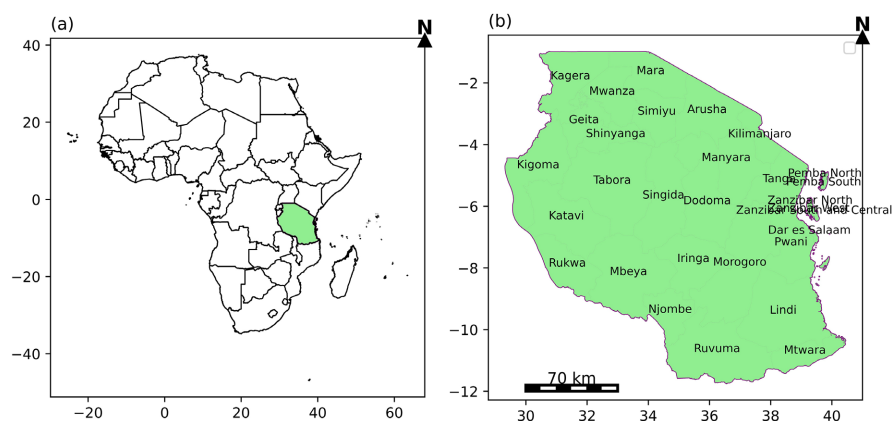


Figure 1. (a) The tanzania's position on the african map; (b) 30 Regions for which its data were used for the study.

2.2.2. Dipole Mode Index

Monthly Dipole Mode Index (DMI) data (1993–2023) were retrieved to assess the influence of the Indian Ocean Dipole (IOD) on rainfall onset. The classification of positive and negative IOD events is based on the differences in sea surface temperature (SST) gradients between the western (50°E – 70°E , 10°S – 10°N) and eastern (90°E – 110°E , 10°S – 0°N) equatorial Indian Ocean. The dataset consists of monthly mean values presented on a $2.5^{\circ} \times 2.5^{\circ}$ grid. Previous studies, including those by [24] and [14], have also employed this dataset for similar analyses and the data were accessed from the Royal Netherlands Meteorological Institute (KNMI) Climate Explorer and is accessible at [http://climexp.knmi.nl/data/ihadisst1_dmi.dat].

2.2.3. Niño 3.4

The Niño 3.4 index, representing sea surface temperature anomalies over the equatorial Pacific (5°S – 5°N and 170°W – 120°W), was obtained from NOAA's Climate Prediction Center consists of monthly mean values with a resolution of $2.5^{\circ} \times 2.5^{\circ}$. SOI data, which indicate pressure differences between Tahiti (17.5°S , 149.6°W) and Darwin (12.4°S , 130.9°E), were sourced from the National Centers for Environmental Prediction (NCEP) and analyzed using an approach similar to that employed by [25].

2.2.4. Atmospheric Circulation Data

Monthly reanalysis data, including meridional (V) and zonal (U) wind components, velocity potential, and vertical velocity, were obtained from the NCEP/NCAR reanalysis project to assess large-scale atmospheric patterns associated with early and late onset events as previously applied in studies such as [26].

2.3. Methods

2.3.1. Empirical Orthogonal Function Analysis

The study used the Empirical Orthogonal function (EOF) analysis to examine spa-

tial and temporal variability in rainfall onset dates across Tanzania. This method decomposes variability into orthogonal modes, identifying dominant patterns in the dataset [27]. The principal component (PC) associated with the leading EOF mode was used to represent onset date variability, with raw data detrended prior to analysis as used by [28].

2.3.2. Composite Analysis

Composite analysis was also employed in this study in order to assess atmospheric anomalies during years of Early Onset Date (EOD) and Late Onset Date (LOD) events. The principle behind this approach is that when data are averaged in relation to a particular event, the event's signal remains prominent while other influences tend to cancel out [29]. The approach involved; Classifying years into EOD, LOD, and normal onset years. Computing the mean anomalies of circulation parameters (e.g., wind patterns, vertical velocity, and velocity potential as done by [30] for EOD and LOD years. Identifying large-scale convergence and divergence patterns influencing OND rainfall onset.

2.3.3. Correlation Analysis

Pearson's correlation coefficient (r) was used to quantify relationships between rainfall onset dates and climate indices (Niño 3.4 and DMI) as conducted by [31]. The correlation coefficient was calculated using:

$$r_{xy} = \frac{n \sum xy - \sum x - \sum y}{\sqrt{\{n \sum x^2 - (\sum x)^2\} \{n \sum y^2 - (\sum y)^2\}}} \quad (1)$$

where “ x ” represents onset dates and “ y ” denotes climate index values. A statistical significance test was performed using a two-tailed t -test at a 95% confidence level.

To assess the statistical significance of the computed correlation coefficient, a two-tailed t -test was applied, as expressed in the equation below:

$$t = \frac{r_{xy} \sqrt{n-2}}{1 - (r_{xy})^2} \quad (2)$$

3. Results

3.1. Climatology of the Spatiotemporal Distribution

A single criterion was applied to determine rainfall onset dates, which was based on the number of rainy days and dry spells. Specifically, a threshold of 1.0 mm of rainfall per day was considered a “rainy day,” with days below this threshold classified as “dry days” [32]. The onset date was defined as the first day of September with a cumulative total of at least 20 mm of rainfall over four consecutive days, ensuring that at least two of these days were rainy, and no dry spell exceeded 10 days in the following 30 days. This criterion was adapted from previous studies [18] [33] [34]. The analysis of rainfall onset dates (1993–2023) revealed significant variations across Tanzania's climatic zones, with both EOD and LOD patterns. Early onset is more common in the Lake Victoria Basin (LVB) and northern

coastal areas. The earliest onset was recorded in Manyara, where rainfall begins in the second decade of August. In bimodal regions, the second rainfall season starts earlier in Manyara, parts of the LVB, and the Northern East Highlands (NEH), typically in August or early September. In contrast, other areas within the same regime experience a later onset. **Figure 2** illustrates these spatial and temporal variations in rainfall onset dates.

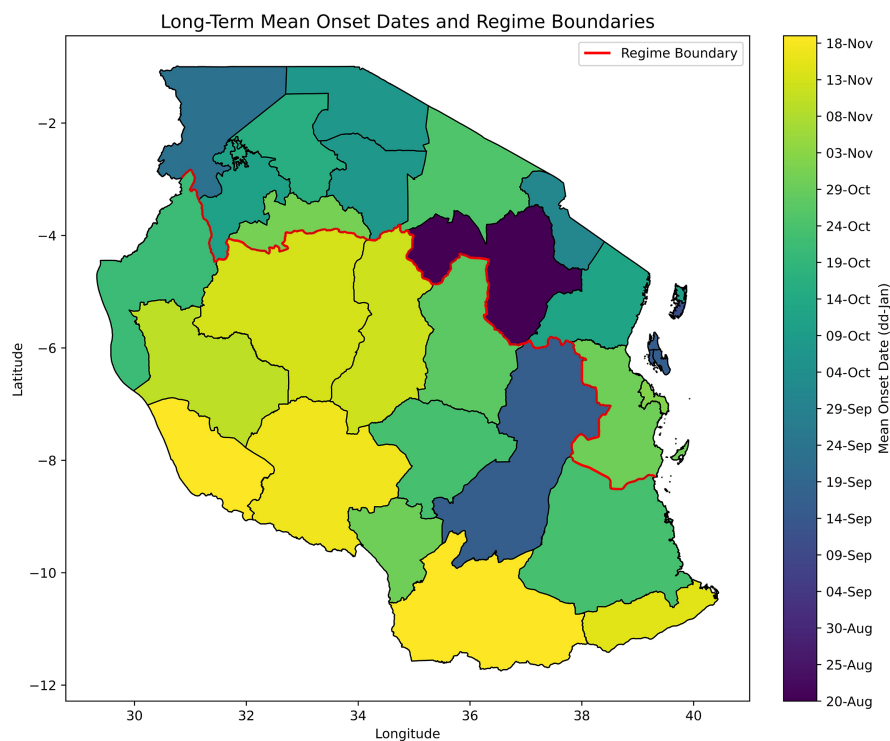


Figure 2. The long term means spatiotemporal distribution of Rainfall onset dates with 10 days or more dry spells, The red line is a regime boundary line that separates areas that experience two rainy seasons (bimodal at the top) and one rainy season (unimodal at the bottom).

In areas with a unimodal rainfall regime, such as the Southern, Southern Coast, and Southwestern Highlands, rainfall onset typically occurs later, around November or December. Some regions, like those near Lake Tanganyika and in the Southwestern Highlands, experience onset between late October and mid-November. Extreme early onset patterns were observed in Manyara and parts of southern Morogoro, where rainfall begins as early as August 20th to September 19th. However, regions with intermittent rainfall experienced disruptions, with dry spells affecting the reliability of onset dates.

3.2. The Variation Modes of Rainfall Onset Dates

The spatiotemporal variability of rainfall onset dates was analyzed using Empirical Orthogonal Function (EOF) analysis to identify regions prone to EOD and LOD. EOF-1 (**Figure 3(a)**) explains 28.0% of the total variance, highlighting key pat-

terns of onset variability. The principal component (PC1) time series (**Figure 3(b)**) tracks the strength of this pattern over time. Years with a standardized mean onset departure of +1 or more (significantly delayed onset) include 1993, 1996, 1998, 2003, 2016, and 2021, while those with departures of -1 or less (significantly early onset) occurred in 1994, 1997, 1999, 2000, 2002, 2004, 2006, 2007, 2008, 2009, 2010, 2011, and 2012.

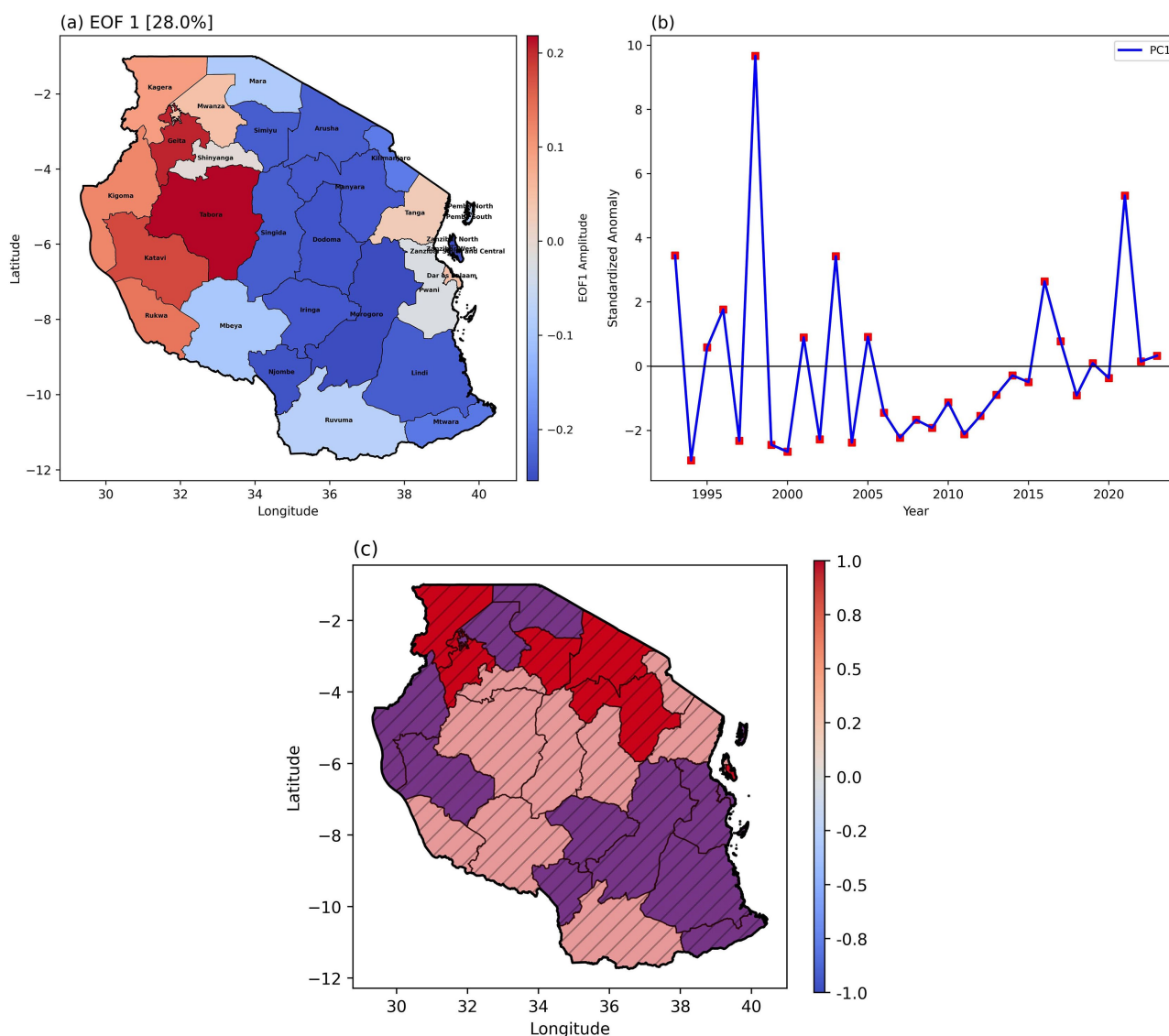


Figure 3. (a) First EOF mode spatial pattern, (b) PC-1 time series for the first EOF mode of OND onset dates, and (c) Composite difference of onset days between LOD and EOD. Red indicates positive differences, purple negative, and light colors show weak/neutral differences. Hatch-marked areas are statistically significant at the 95% confidence level.

The spatial pattern of EOF-1 (**Figure 3(a)**) shows that the western and north-eastern parts of the study domain tend to experience later onset dates, as indicated by positive loadings. In contrast, areas in the Northern East Highlands (NEH), central regions (Singida and Dodoma), and southern regions (Ruvuma, Mtwara,

Njombe, Iringa, and Morogoro) are more likely to have earlier onset dates, as indicated by negative loadings. Notably, positive loadings are most pronounced over the Lake Victoria Basin (LVB), especially in the southern and western areas, as well as in the western regions (Tabora and Kigoma), the northern coast (Tanga, Dar es Salaam, and Pwani), and parts of the Southwestern Highlands (SWH), including Rukwa and Katavi.

Figure 3(c) shows red-shaded regions (positive composite difference) where late onset years have significantly delayed rainfall compared to early onset years. Significant delays in LOD years (red-shaded) were observed in the western and eastern Lake Victoria Basin (LVB), the northern coast, and parts of the Northern East Highlands (NEH). Earlier onset (purple-shaded) occurred in the Southwestern Highlands (SWH), coastal regions, and western zone areas like Morogoro and Kigoma. Hatch-marked areas are statistically significant ($p < 0.0001$), indicating non-random differences. This dipole-like variability suggests that large-scale processes, such as regional circulation, the Indian Ocean Dipole (IOD), and ENSO, influence rainfall onset.

3.3. Larger Scale Circulation Patterns

Figure 4 illustrates composite wind patterns at 200 hPa and 850 hPa during Late Onset Date (LOD) and Early Onset Date (EOD) years, along with their differences. During LOD years, the upper-level circulation (**Figure 4(a)**) is characterized by strong anomalous westerlies, including northwesterly and southwesterly flows that converge over East Africa. This convergence aloft is indicative of subsiding motion, which suppresses the development of deep convection. At the lower troposphere (850 hPa; **Figure 4(b)**), anomalous easterly winds dominate, accompanied by divergence over the region. The presence of persistent easterlies from the Congo Basin further inhibits low-level moisture convergence. This vertical wind structure—upper-level convergence and low-level divergence creates an unfavorable environment for vertical ascent, thereby delaying the onset of rainfall.

In contrast, EOD years exhibit a reversed pattern. At 200 hPa (**Figure 4(d)**), easterly wind anomalies with divergent flow prevail over Tanzania, promoting upper-level outflow and facilitating the development of convective towers. Meanwhile, at 850 hPa (**Figure 4(e)**), anomalous westerlies enhance low-level moisture transport from the Congo Basin and the tropical Atlantic, resulting in convergence over the region. This configuration supports ascending motion and enhanced convection, thereby favoring an earlier onset of rainfall. The difference fields (**Figure 4(c)** and **Figure 4(f)**) further emphasize these contrasting circulation patterns, with significant anomalies in both upper and lower tropospheric winds between LOD and EOD years. These results highlight the importance of vertically coherent large-scale circulation in modulating the timing of seasonal rainfall onset over East Africa.

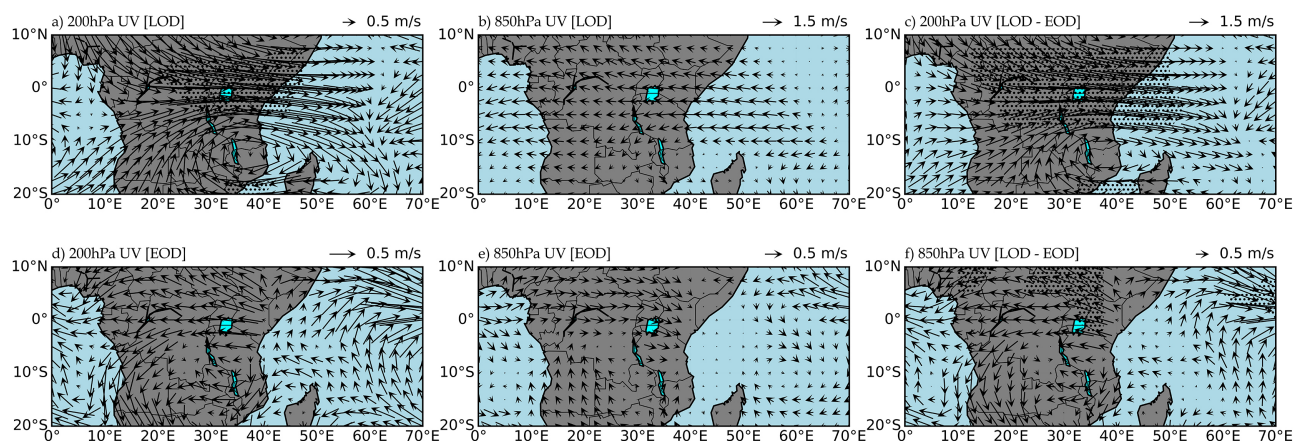


Figure 4. Wind anomalies at 200 hPa and 850 hPa for LOD ((a) (b)) and EOD ((c) (d)), with differences at (e) 850 hPa and (f) 200 hPa and hatched areas denote statistical significance (95% confidence).

3.4. Distribution of Sea Surface Temperature Anomaly

The analysis in **Figure 5(a)** highlights statistically significant regions of sea surface temperature anomaly (SSTA) between LOD and EOD years. The southwestern Indian Ocean (south of 10°S) experiences pronounced cooling, whereas the central and eastern Indian Ocean exhibit warming. These findings suggest that the timing of IOD and Niño 3.4 plays a crucial role in the rainfall onset date. The stronger cooling in the southwestern Indian Ocean may have implications for regional climate conditions, including enhanced suppression of convection over the western Indian Ocean and potential modifications to Walker Circulation anomalies. This

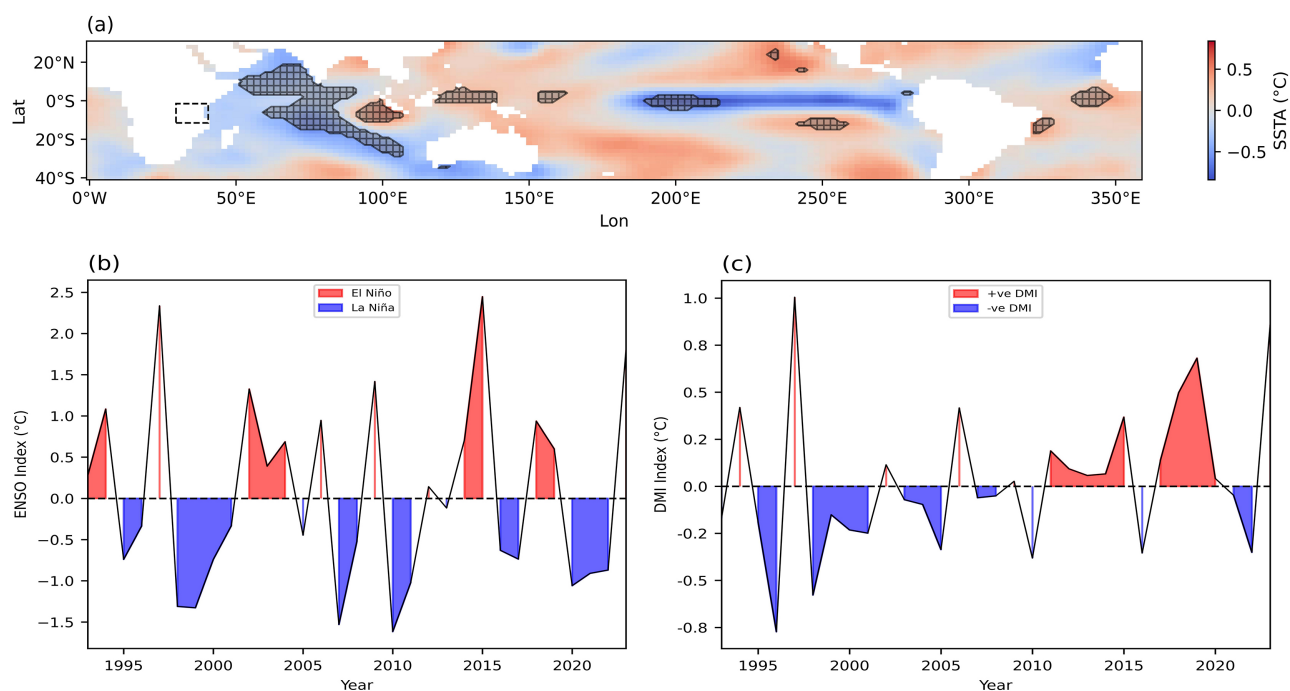


Figure 5. (a) Spatial distribution of SSTA differences between LOD and EOD with those areas at 95% confidence level (hatched region). The time series of (b) ENSO Index (Niño 3.4 anomaly) and (c) DMI for the OND season from 1993 to 2023.

could influence rainfall patterns over East Africa, the Maritime Continent, and Australia, regions that are heavily affected by IOD and Niño 3.4-driven variability. Moreover, warmer/cold SSTs in the eastern Indian Ocean, cold/warmer SSTs in western Indian and eastern Pacific could induce ascending/descending motion over the region, and enhance/weaken moisture availability, affecting the rainfall onset day in surrounding regions.

The two panels (b and c) in the **Figure 5** illustrate the interannual variability of the Niño 3.4 index and the DMI during the OND season. Both indices have marked inter-annual variation, and the typical years are defined for further study the relationship between onset day over the region and the ENSO/IOD. The years with standard anomaly indices of the threshold $+0.5$ or more (El Niño) include 1994, 1997, 2002, 2004, 2006, 2009, 2014, 2015, 2018, 2019 and 2023 while those with indices of -0.5 or less (La Niña or Negative Niño 3.4) occurred in 1995, 1998, 1999, 2000, 2007, 2008, 2010, 2011, 2016, 2017, 2020, 2021 and 2022. On the other hand, for the DMI, the years with standard anomaly indices of the threshold $+0.4$ or more were 1994, 1997, 2006, 2018, 2019 and 2023 while those with indices of -0.4 or less occurred in 1996 and 1998.

3.5. Drivers for Larger Scale Patterns

The Relationship between Climate Indices and Rainfall Onset across Tanzania

This section examines the relationship between inter-annual rainfall onset dates and climatic indices, specifically Niño 3.4 and the Dipole Mode Index (DMI), shown through spatial maps (**Figure 6**) at the 95% confidence level during the OND season over Tanzania. Correlation results in **Figure 6** show the correlation patterns of the two indices are similar, with positive coefficients in the middle and eastern part of the country, while negative ones in northwest and part of the east.

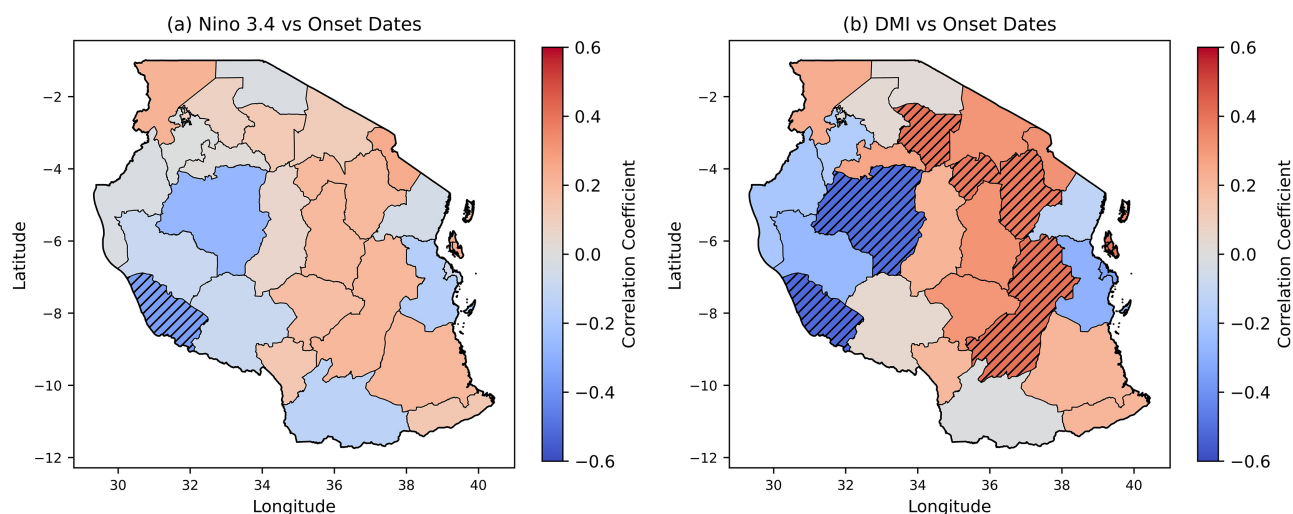


Figure 6. The correlation coefficients between rainfall onset dates and (a) Niño 3.4 and (b) Indian Ocean Dipole Mode Index (DMI). Red shades indicate positive correlations (earlier onset with increasing index values), while blue shades indicate negative correlations (delayed onset with increasing index values).

The Nino 3.4 index, representing warm temperature anomalies in the central Pacific (linked to ENSO), shows correlations (**Figure 6(a)**) with rainfall onset across areas like Kilimanjaro, Zanzibar, and Iringa (e.g., Kilimanjaro, $r = 0.239$) exhibiting positive correlations, suggesting that warmer Pacific temperatures, indicative of El Niño, delaying rainfall onset over north and central areas. In contrast, regions like Rukwa and Tabora ($r = -0.357$ and $r = -0.268$) show negative correlations, where El Niño accelerates rainfall onset.

The DMI (Dipole Mode Index), which measures the temperature difference between the western and eastern Indian Ocean, plays a more dominant role in influencing rainfall onset in Tanzania. Correlations in **Figure 6(b)** range from $r = -0.517$ (Rukwa) to $r = 0.407$ (Simiyu), indicating that the Indian Ocean's warming and cooling patterns have a stronger and more consistent effect on rainfall timing. A positive IOD event, earlier rainfall onset in regions like Rukwa and Tabora will be induced. In contrast, a negative IOD will delay rainfall, especially in central and northern Tanzania. This suggests that Indian Ocean variability is more influential than ENSO in shaping Tanzania's rainfall onset date. And from the correlation coefficients, the ones with Niño 3.4 are less than those with DMI, indicating more important role play by Indian Dipole on the rainfall onset day.

To further interpret the observed correlations, it is essential to explore the underlying physical mechanisms by which SST anomalies influence rainfall onset over Tanzania. El Niño events (positive Niño 3.4 anomalies) alter the Walker Circulation, shifting convection toward the central and eastern Pacific. This shift suppresses convection over the western Pacific and East Africa, leading to subsidence and reduced moisture availability. As a result, rainfall onset is often delayed in northern and central Tanzania during El Niño years. In contrast, La Niña tends to enhance convection over the western Indian Ocean and East Africa, promoting earlier rainfall onset in those regions. The Indian Ocean Dipole (IOD), represented by the DMI, exerts a more direct and often stronger influence. Positive IOD events, characterized by warmer western Indian Ocean SSTs and cooler eastern SSTs, enhance the west-east SST gradient. This intensifies the equatorial westerlies and facilitates moisture flux convergence over East Africa, which strengthens convection and typically leads to earlier rainfall onset, especially in western and central Tanzania. Negative IOD phases weaken this gradient, reducing moisture inflow and delaying the onset of rains.

3.6. Circulation Influenced by Tropical Drivers

3.6.1. Circulation Patterns

As denoted above, both ENSO and IOD can influence the rainfall onset day. Then how do ENSO and IOD affect the rainfall onset? Here composite analysis on the circulation patterns for typical ENSO and IOD years. Wind anomalies during positive/negative indices years look similar in some features like that of **Figure 4**, revealing the circulation patterns associated rainfall onset day able to be induced by ENSO and IOD. That is, stronger easterly winds with convergence at 200 hPa, and

westerly winds with divergence at 850 hPa can be induced by warm SSTA in eastern0central Pacific and western Indian Ocean during positive index years, delaying rainfall onset day over most part of the region, especially over east part of the region. However, the composite circulation over negative years will making rainfall onset earlier over most part of the region.

3.6.2. Rainfall Onset Day

Figure 7 illustrates the impact of ENSO and IOD on rainfall onset dates during the OND season in Tanzania. **Figure 7(a)** shows that Niño 3.4 does not significantly affect onset dates (T-statistic = -0.90, p-value = 0.3807), indicating a weak ENSO influence. In contrast, **Figure 7(b)** highlights the significant role of DMI (T-statistic = -2.58, p-value = 0.0196), with regions in red indicating late onset and those in purple/pink showing earlier onset. As DMI significantly influences rainfall timing, monitoring IOD variations is crucial for stakeholders planning for the rainy season.

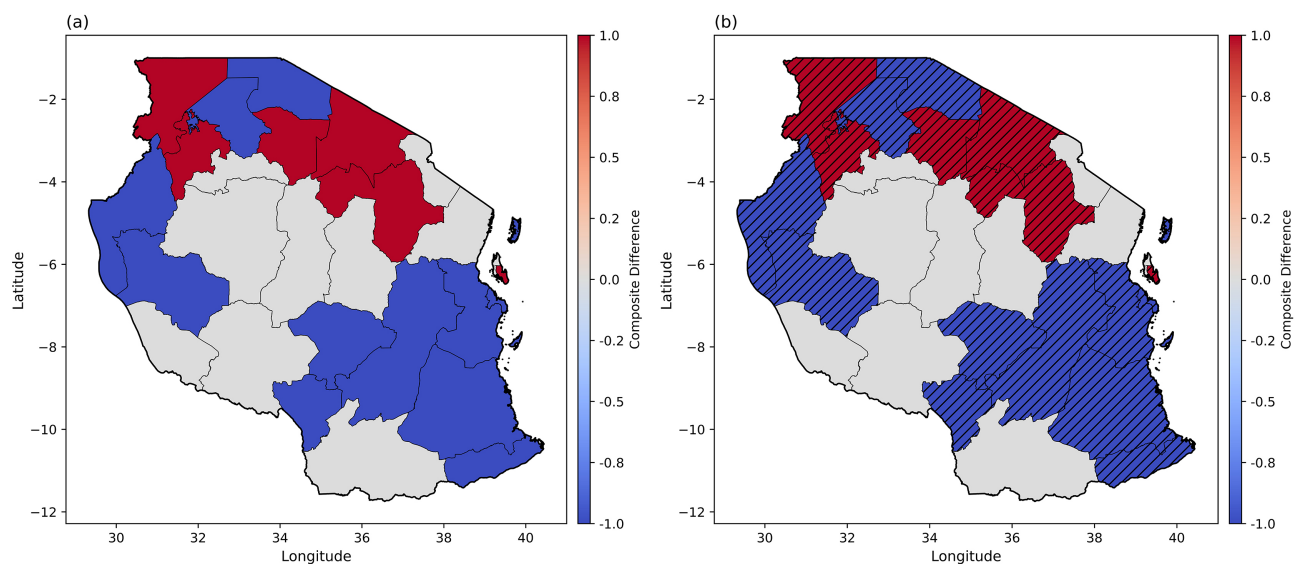


Figure 7. Composite differences of the onset days between positive and negative indices years (a) influenced by Niño 3.4 (b) influenced by DMI during the OND rainfall. Shattered areas are exceeding t-test at 95% confidence level.

The regions most affected by ENSO and IOD are the central and northern parts, where the onset of the OND rains is particularly sensitive to large-scale atmospheric conditions. For instance, in central and north Tanzania, including areas like Kilimanjaro and Arusha, El Niño years/positive IOD often result in the earliest rains, whereas La Niña/negative IOD years see a delayed rainfall onset date there.

4. Conclusions and Discussion

This study has analyzed the inter-annual variation of the onset date during the OND rainfall season in Tanzania, with a particular focus on spatial and temporal variations, circulation anomalies, and key forcing factors.

The onset dates were determined using a threshold-based method, while spatial and temporal variability was analyzed through Empirical Orthogonal Function analysis. In Tanzania, there is a unimodal rainfall regime, such as the Southern, Southern Coast, and Southwestern Highlands, rainfall onset typically occurs later, around November or December. The spatial pattern of EOF-1 shows similar to the climatology, that is, the rainfall onset day over most part of the country is opposite (later/earlier) to that (earlier /later) on the northwest and southeast.

Key findings show that during LOD years, anomalous easterly upper-level winds with convergence and westerly lower-level winds with divergence at low-level, suppress moisture transport with descending over the region will delay rainfall onset. In contrast, the opposite anomaly circulation during EOD years will result in earlier rainfall onset.

Both ENSO and IOD have close relationship with the rainfall onset day in Tanzania. Warm SSTA in eastern-central Pacific and western Indian Ocean during El Niño years/positive IOD years, can induce LOD associated circulation patterns and then delay rainfall onset day over most part of the region, especially over east part of the region. However, the warm SSTA in western Pacific to eastern Indian Ocean during La Niña/negative IOD years will induce EOD-like circulation patterns, which will make rainfall onset earlier over most part of the country.

In this study, only the large-scale circulation of rainfall onset day in Tanzania and associated tropical drivers are investigated. And how do the tropical drivers influence the local circulation and moisture condition remain unclear. Other important drivers apart from ENSO and IOD such as the Madden-Julian Oscillation (MJO) and sub-seasonal shifts of the Intertropical Convergence Zone (ITCZ) were not included. These factors operate on shorter timescales and can significantly affect the timing and spatial variability of rainfall onset. Further study should incorporate such intraseasonal dynamics to provide a more comprehensive understanding of the mechanisms influencing seasonal rainfall patterns in the region.

Acknowledgements

The first author appreciates acknowledging the Government of Tanzania for providing opportunity to carry on with studies and the Ministry of Commerce of China (MOFCOM) for sponsorship. Many thanks to Prof. Tan Guirong for supervising and guiding this research. Many thanks to CHIRPS, ECMWF-ERA5, NOAA and Tanzania Meteorological Authority for data availability.

Conflicts of Interest

The authors declare no conflict of interest regarding the publication of this paper.

References

- [1] Calvin, K., Dasgupta, D., Krinner, G., Mukherji, A., Thorne, P.W., Trisos, C., Romero, J., Aldunce, P., *et al.* (2023) IPCC, 2023: Climate Change 2023: Synthesis Report. Contribution of Working Groups I, II and III to the Sixth Assessment Report of

- the Intergovernmental Panel on Climate Change.
- [2] Min, S., Zhang, X., Zwiers, F.W. and Hegerl, G.C. (2011) Human Contribution to More-Intense Precipitation Extremes. *Nature*, **470**, 378-381. <https://doi.org/10.1038/nature09763>
 - [3] Royal Society, T. Climate Change: Evidence & Causes 2020. <https://www.nap.edu/catalog/18373>
 - [4] Dai, A. (2013) Increasing Drought under Global Warming in Observations and Models. *Nature Climate Change*, **3**, 52-58. <https://doi.org/10.1038/nclimate1633>
 - [5] Seager, R., Neelin, D., Simpson, I., Liu, H., Henderson, N., Shaw, T., *et al.* (2014) Dynamical and Thermodynamical Causes of Large-Scale Changes in the Hydrological Cycle over North America in Response to Global Warming. *Journal of Climate*, **27**, 7921-7948. <https://doi.org/10.1175/jcli-d-14-00153.1>
 - [6] Wani, S.P., Sreedevi, T.K., Rockström, J. and Ramakrishna, Y.S. (2009) Rainfed Agriculture-Past Trends and Future Prospects. In: Wani, S.P., Rockström, J. and Oweis, T., Eds., *Rainfed agriculture. Unlocking the Potential*, CABI, 1-35. <https://doi.org/10.1079/9781845933890.0001>
 - [7] Ahmad, I., Tang, D., Wang, T., Wang, M. and Wagan, B. (2015) Precipitation Trends over Time Using Mann-Kendall and Spearman's Rho Tests in Swat River Basin, Pakistan. *Advances in Meteorology*, **2015**, Article 431860. <https://doi.org/10.1155/2015/431860>
 - [8] Arndt, C., Chinowsky, P., Robinson, S., Strzepek, K., Tarp, F. and Thurlow, J. (2012) Economic Development under Climate Change. *Review of Development Economics*, **16**, 369-377. <https://doi.org/10.1111/j.1467-9361.2012.00668.x>
 - [9] Ayugi, B., Eresanya, E.O., Onyango, A.O., Ogou, F.K., Okoro, E.C., Okoye, C.O., *et al.* (2022) Review of Meteorological Drought in Africa: Historical Trends, Impacts, Mitigation Measures, and Prospects. *Pure and Applied Geophysics*, **179**, 1365-1386. <https://doi.org/10.1007/s00024-022-02988-z>
 - [10] Kai, K.H., Kijazi, A.L., Osima, S.E., Mtongori, H.I., Makame, M.O., Bakari, H.J., *et al.* (2021) Spatio-Temporal Assessment of the Performance of March to May 2020 Long Rains and Its Socio-Economic Implications in Northern Coast of Tanzania. *Atmospheric and Climate Sciences*, **11**, 767-796. <https://doi.org/10.4236/acs.2021.114045>
 - [11] Mpelasoka, F., Hennessy, K., Jones, R. and Bates, B. (2007) Comparison of Suitable Drought Indices for Climate Change Impacts Assessment over Australia Towards Resource Management. *International Journal of Climatology*, **28**, 1283-1292. <https://doi.org/10.1002/joc.1649>
 - [12] Nicholson, S. (2000) The Nature of Rainfall Variability over Africa on Time Scales of Decades to Millennia. *Global and Planetary Change*, **26**, 137-158. [https://doi.org/10.1016/s0921-8181\(00\)00040-0](https://doi.org/10.1016/s0921-8181(00)00040-0)
 - [13] Camberlin, P., Moron, V., Okoola, R., Philippon, N. and Gitau, W. (2009) Components of Rainy Seasons' Variability in Equatorial East Africa: Onset, Cessation, Rainfall Frequency and Intensity. *Theoretical and Applied Climatology*, **98**, 237-249. <https://doi.org/10.1007/s00704-009-0113-1>
 - [14] Saji, N.H., Goswami, B.N., Vinayachandran, P.N. and Yamagata, T. (1999) A Dipole Mode in the Tropical Indian Ocean. *Nature*, **401**, 360-363. <https://doi.org/10.1038/43854>
 - [15] Luhunga, P.M., Mutayoba, E. and Ng'ongolo, H.K. (2014) Homogeneity of Monthly Mean Air Temperature of the United Republic of Tanzania with Homer. *Atmospheric and Climate Sciences*, **4**, 70-77. <https://doi.org/10.4236/acs.2014.41010>
 - [16] Linderholm, H.W., Nicolle, M., Francus, P., Gajewski, K., Helama, S., Korhola, A., *et*

- al.* (2018) Arctic Hydroclimate Variability during the Last 2000 Years: Current Understanding and Research Challenges. *Climate of the Past*, **14**, 473-514. <https://doi.org/10.5194/cp-14-473-2018>
- [17] Japheth, L.P., Tan, G., Chang'a, L.B., Kijazi, A.L., Mafuru, K.B. and Yonah, I. (2021) Assessing the Variability of Heavy Rainfall during October to December Rainfall Season in Tanzania. *Atmospheric and Climate Sciences*, **11**, 267-283. <https://doi.org/10.4236/acs.2021.112016>
- [18] Recha, C.W., Makokha, G.L., Traore, P.S., Shisanya, C., Lodoun, T. and Sako, A. (2012) Determination of Seasonal Rainfall Variability, Onset and Cessation in Semi-Arid Tharaka District, Kenya. *Theoretical and Applied Climatology*, **108**, 479-494. <https://doi.org/10.1007/s00704-011-0544-3>
- [19] GIZ (2021) Home-Deutsche Gesellschaft für Internationale Zusammenarbeit (GIZ) GmbH-Integrated Company Report 2021. <https://reporting.giz.de/2021/>
- [20] Kabanda, T. (2018) Long-Term Rainfall Trends over the Tanzania Coast. *Atmosphere*, **9**, Article 155. <https://doi.org/10.3390/atmos9040155>
- [21] Mbululo, Y. and Nyihirani, F. (2012) Climate Characteristics over Southern Highlands Tanzania. *Atmospheric and Climate Sciences*, **2**, 454-463. <https://doi.org/10.4236/acs.2012.24039>
- [22] Funk, C., Peterson, P., Landsfeld, M., Pedreros, D., Verdin, J., Shukla, S., *et al.* (2015) The Climate Hazards Infrared Precipitation with Stations—A New Environmental Record for Monitoring Extremes. *Scientific Data*, **2**, Article No. 150066. <https://doi.org/10.1038/sdata.2015.66>
- [23] Muthoni, F.K., Odongo, V.O., Ochieng, J., Mugalavai, E.M., Mourice, S.K., Hoesche-Zeledon, I., *et al.* (2019) Long-Term Spatial-Temporal Trends and Variability of Rainfall over Eastern and Southern Africa. *Theoretical and Applied Climatology*, **137**, 1869-1882. <https://doi.org/10.1007/s00704-018-2712-1>
- [24] Muhati, F., Ininda, J.M. and Opijah, F.J. (2007) Relationship Between ENSO Parameters and the Trends and Periodic Fluctuations in East African Rainfall. *Journal of the Kenya Meteorological Society*, **1**, 20-43.
- [25] Jury, M.R. and Levey, K. (1993) The Climatology and Characteristics of Drought in the Eastern Cape of South Africa. *International Journal of Climatology*, **13**, 629-641. <https://doi.org/10.1002/joc.3370130604>
- [26] Kalnay, E., Kanamitsu, M., Kistler, R., Collins, W., Deaven, D., Gandin, L., *et al.* (1996) The NCEP/NCAR 40-Year Reanalysis Project. *Bulletin of the American Meteorological Society*, **77**, 437-471. [https://doi.org/10.1175/1520-0477\(1996\)077<0437:tnyrp>2.0.co;2](https://doi.org/10.1175/1520-0477(1996)077<0437:tnyrp>2.0.co;2)
- [27] Bjornsson, H. and Venegas, S.A. (1997) A Manual for EOF and SVD Analyses of Climate Data. *CCGCR Report No. 97-1*, Climate Research Branch, Environment Canada, 52 p.
- [28] Hotelling, H. (1933) Analysis of a Complex of Statistical Variables into Principal Components. *Journal of Educational Psychology*, **24**, 417-441. <https://doi.org/10.1037/h0071325>
- [29] Hartmann, D.L. (2008) Compositing or Superposed Epoch Analysis. 35-37.
- [30] Indeje, M., Semazzi, F.H.M. and Ogallo, L.J. (2000) ENSO Signals in East African Rainfall Seasons. *International Journal of Climatology*, **20**, 19-46. [https://doi.org/10.1002/\(sici\)1097-0088\(200001\)20:1<19::aid-joc449>3.0.co;2-0](https://doi.org/10.1002/(sici)1097-0088(200001)20:1<19::aid-joc449>3.0.co;2-0)
- [31] Asuero, A.G., Sayago, A. and González, A.G. (2006) The Correlation Coefficient: An Overview. *Critical Reviews in Analytical Chemistry*, **36**, 41-59.

- <https://doi.org/10.1080/10408340500526766>
- [32] Ojara, M.A., Lou, Y., Aribi, L., Namumbya, S. and Uddin, M.J. (2020) Dry Spells and Probability of Rainfall Occurrence for Lake Kyoga Basin in Uganda, East Africa. *Natural Hazards*, **100**, 493-514. <https://doi.org/10.1007/s11069-019-03822-x>
- [33] Marteau, R., Moron, V. and Philippon, N. (2009) Spatial Coherence of Monsoon Onset over Western and Central Sahel (1950-2000). *Journal of Climate*, **22**, 1313-1324. <https://doi.org/10.1175/2008jcli2383.1>
- [34] Stern, R. (2006) Instat Climatic Guide. <https://www.researchgate.net/publication/264879427>